The microbiota promotes social behavior by neuro-immune modulation of neurite complexity

Joseph J. Bruckner[1], Sarah J. Stednitz[2], Max Z. Grice[1], Johannes Larsch[3], Alexandra Tallafuss[1], Philip Washbourne[1]*, Judith S. Eisen[1]*

Author affiliations

[1]Institute of Neuroscience, Department of Biology, University of Oregon, Eugene, OR 97403, USA

[2]Department of Sensory & Sensorimotor Systems, Max Planck Institute for Biological Cybernetics, 72076, Tübingen, Germany

[3]Department Genes-Circuits-Behavior, Max Planck Institute of Neurobiology, 82152, Martinsried, Germany

*corresponding author

Abstract

Host-associated microbiotas normally guide the trajectory of intrinsically encoded developmental programs, and dysbiosis is linked to neurodevelopmental disorders such as autism spectrum disorder. Recent work suggests that microbiotas modulate social phenotypes associated with these disorders, though developmental mechanisms linking microbiotas to social behavior are not well understood. We discovered that the zebrafish microbiota is required for normal social behavior. Using this model to examine neuronal features modulated by the microbiota during early development, we found that the microbiota restrains neurite complexity and targeting of specific forebrain neurons required for normal social behavior. The microbiota is also required for normal forebrain infiltration of microglia, the brain's resident phagocytes that remodel neuronal arbors, suggesting the microbiota modulates arborization via a neuro-immune route. Our work establishes a foundation for study of microbial and host mechanisms that link the microbiota and social behavior in an experimentally tractable model vertebrate.

Introduction

Impaired social behavior is a hallmark of multiple neurodevelopmental disorders, including autism spectrum disorder (ASD) and schizophrenia.[1] However, the organization, function, and development of the brain circuits underlying social interactions are poorly understood, and effective interventions in these disorders are elusive. Zebrafish are an excellent model for understanding development of the social brain and generating insights to inform interventions in humans. Development of the early circuitry that regulates mammalian social behavior is difficult to observe in the prenatal brain, whereas equivalent neurodevelopment is readily visualized *in vivo* in transparent larval zebrafish. Zebrafish are naturally gregarious, and manifest social traits including shoaling, aggression, kin recognition, and orienting as early as 12-16 days post fertilization (dpf).[2–7] Combining the genetic and experimental accessibility of zebrafish, we can identify precise developmental events that facilitate normal social behavior and that may go awry in neurodevelopmental disorders.

Previous work suggests that the zebrafish ventral nucleus of the ventralis telencephali (Vv) is required for normal social behaviors including mating, place preference, and orienting.[3,8,9] This region of the zebrafish brain is part of a circuit that is homologous to subpallial regions of the mammalian brain that also regulate social behavior, including the lateral septum, preoptic area, and hypothalamus.[10–12] Connectomic studies suggest that Vv may have an integrative function, receiving afferent input from the midbrain and olfactory bulb and sending efferent projections to higher-order processing centers including the habenula and hypothalamus.[10–12] Our previous work identified a subpopulation of Vv neurons required for normal zebrafish social orienting and place preference. This subpopulation is defined by partial enhancer trap of *lhx8a*, which encodes a transcription factor involved in regulating neurotransmitter identity.[13] For simplicity we refer to this subpopulation of the ventral telencephalon according to the Gal4 enhancer trap transgene that labels it, y321 (vTel^{y321}).[14] The neuronal features that facilitate normal circuit connectivity are likely established long before social orienting is expressed at 14 dpf, so the rapid, sequential development of social characteristics could represent ongoing

refinement of cells and circuits that execute social behavior.[2] For example, development of many neuronal circuits is characterized by a critical period of initial outgrowth and synapse formation followed by pruning of superfluous connections and strengthening of specific nodes. Therefore, understanding the intrinsic and extrinsic factors that modify vTel^{y321} circuitry during early development will enable us to predict features that can modify behavioral deficits in social disorders.

It is increasingly appreciated that host-associated microbes can shape social behavior by influencing neurodevelopment.[15] Mice raised germ-free (GF) or with an abnormal microbiota exhibit impaired social behavior, which is correlated with microbial modulation of neuronal gene expression, neurotransmitter levels, brain maturation, and myelination.[16–22] Host-associated microbes influence social behavior across taxa. For example, the *Drosophila melanogaster* microbiota promotes social preference through serotonergic signaling.[23] GF zebrafish have abnormal anxiety-related and locomotor behaviors, which can be attenuated by probiotic administration that also influences shoaling behavior via *brain-derived neurotrophic factor* (*BDNF*) and serotonin signaling.[24–26] However, these *Lactobacillus* strains were applied as a probiotic to adult zebrafish and do not normally populate the zebrafish intestine, so it is unclear whether microbial modulation occurs by this mechanism during normal neurodevelopment of circuits that regulate social behavior.[27,28] Though evidence for a link between microbiota composition and social behavior is abundant across taxa, mechanistic insights require combining access to early development and the ability to manipulate the microbiota in large numbers of genetically similar offspring. Therefore, zebrafish are an ideal model for revealing how the microbiota shapes neurodevelopment and social behavior.

Microglia, the brain's resident myeloid cells, have well-defined roles regulating brain development and function.[29] Microglia modify neuronal morphology by regulating axon outgrowth and refining synapses, and, like many circulating immune cells, are responsive to microbial signals.[29,30] Microglia are also required in the early postnatal brain for development of normal social behavior.[31,32] In vertebrates, microglia infiltrate the brain in multiple waves.[33,34] In zebrafish, this process begins with primitive microglia that differentiate in the rostral blood island, infiltrate the brain around 2.5 dpf, and persist

through larval stages.[35,36] These microglia are eventually replaced by a definitive population that differentiates from hematopoietic stem cells in the dorsal aorta and infiltrates the adult brain beginning at approximately 14 dpf.[34,37] In the larval brain, microglia actively survey the surrounding tissue and phagocytose neuronal material.[38] It is tempting to speculate that the erythromyeloid origins of microglia could generate sensitivity to microbial factors. Consistent with this idea, the microbiota appears to influence normal microglial colonization, maturation, morphology, and activation.[30]

In this study, we use gnotobiotic techniques to identify features of social circuits that require microbiota. First, we found that normal social behavior in late-flexion larvae (around 14 dpf) requires microbes earlier in development, suggesting a critical period for microbial input. We then reconstructed hundreds of individual vTel^{y321} neurons and observed significant microbial modulation of arbor complexity during the period when social behavior is developing. Since microglia are critical for remodeling neurites during circuit development, we tested the hypothesis that the microbiota influences zebrafish forebrain microglia and found that the microbiota promotes forebrain microglial abundance but does not modulate microglial activity. Together, our experiments suggest that the microbiota promotes social behavior by influencing early development of features such as microglial distribution and neuronal arbor targeting.

Results

The microbiota promotes zebrafish social behavior. Conspecific social orienting is apparent at approximately 14 dpf, but neuronal circuits that facilitate this behavior likely develop much earlier. These neurodevelopmental events could be influenced by microbial factors as soon as the intestine becomes patent at approximately 4 dpf (Figure 1a).[2,39] To test the hypothesis that normal social behavior development specifically requires the microbiota early, before social behavior is expressed, we raised zebrafish GF for the first week of life, inoculated with a normal microbiota at 7 dpf, and assessed social behavior at 14 dpf with our previously-described assay of conspecific social orienting (XGF; Figure 1a, b).[3,39] This assay accurately reproduces and measures social orienting behavior exhibited by freely-swimming conspecifics.[2,3] Compared to “conventionalized” siblings derived GF and

then inoculated with a normal microbiota on day zero (CVZ), XGF larvae spend significantly less time than CVZ controls in close proximity to and oriented at 45-90° to face the conspecific stimulus fish

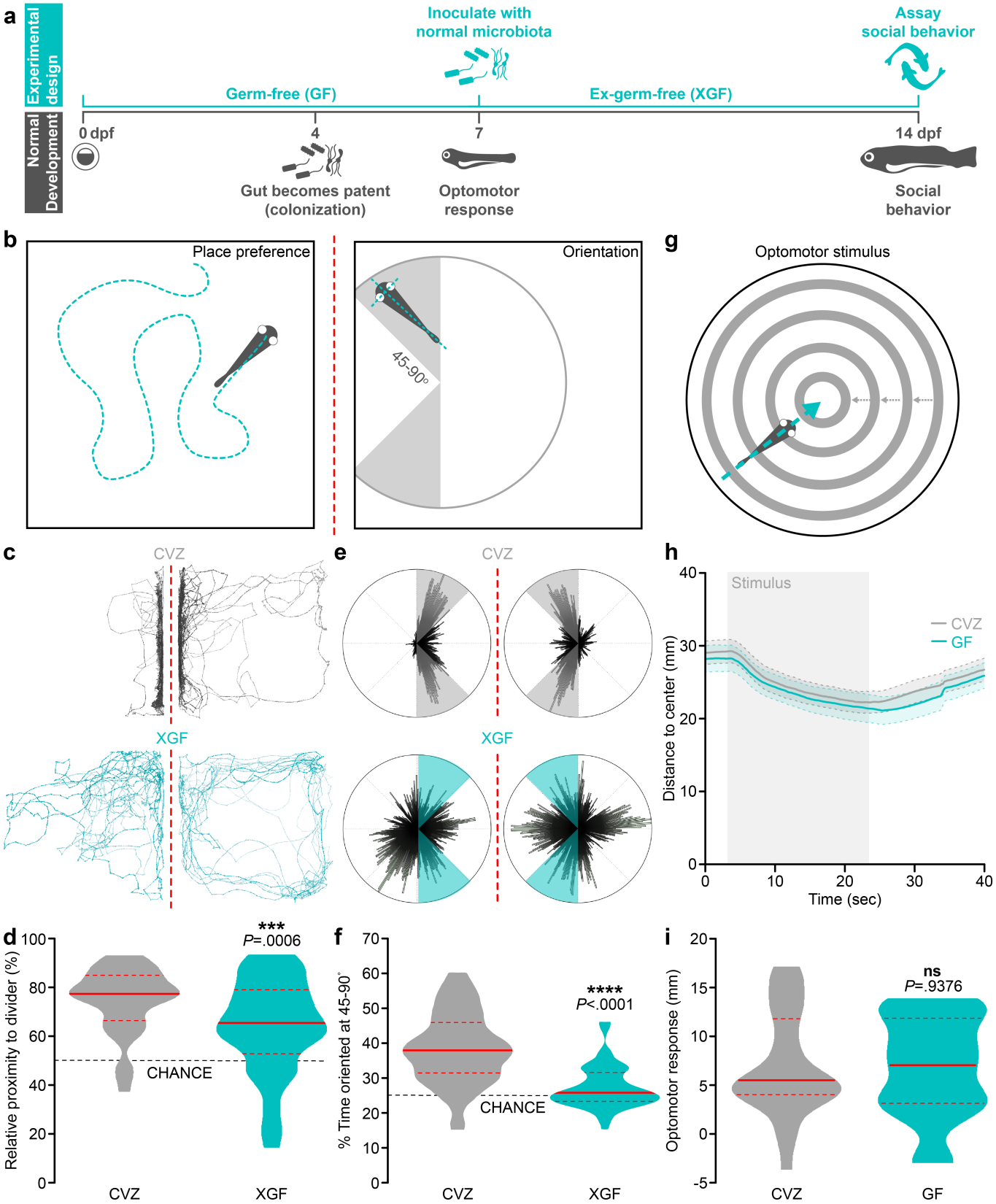

Fig. 1 The microbiota promotes zebrafish social behavior. **a** Experimental design timeline. **b** Zebrafish social behavior is assessed by simultaneously measuring place preference (left) and body orientation (right) in paired fish separated by a transparent divider (dotted red line).[3] **c-f** Social behavior is reduced in 14 dpf XGF larvae relative to CVZ siblings. Traces (**c**) and 360° body position polar plots (**e**) of representative CVZ (gray) and XGF (aqua) larvae during social behavior. Relative proximity to the transparent divider (**d**) and percent of time oriented at 45-90° (**f**) are significantly reduced in XGF (n = 67) larvae relative to CVZ controls (n = 54 larvae; Mann-Whitney U test). **g** Sensorimotor integration is assessed by measuring distance traveled in response to a stimulus simulating motion toward the dish center. **h** Average distance to center is similar in 7 dpf CVZ (gray, n = 25) and GF (aqua, n = 20) larvae during and following stimulus presentation (gray bar; solid lines represent mean, dotted lines represent SEM). **i** Distance traveled in response to optomotor stimulus is not significantly reduced in GF larvae relative to CVZ siblings (Unpaired t-test). ns, not significant; ***, P<.001; ****, P<.0001. Solid red line represents the median, dotted red lines represent the upper and lower quartiles.

(Figure 1c-f, Supplemental movies 1 and 2). Thus, a normal microbiota is required during early stages for later development of normal social behavior.

It is possible that the microbiota does not normally guide social neurodevelopment, but rather that removing the host-associated microbiota for the first week of life causes nutritional deficits that simply delay normal development. Standard length, a commonly used measure of zebrafish development, is slightly but statistically significantly reduced in XGF larvae relative to their CVZ siblings (Figure supplement 1a).[40] To address the possibility that developmental delay accounts for the social deficits in XGF fish, we binned our social orienting measurements according to the standard length of each fish. We do not observe a difference in social orienting between XGF larvae and CVZ siblings that are 5 mm or smaller, likely because these stunted fish are unable to execute social orienting. However, social orienting remains decreased in XGF larvae size matched to CVZ controls that are 6 mm or longer (Figure supplement 1b). Smaller standard length is significantly correlated with reduced orienting behavior (P=.02). However, when treatment condition is considered as a covariate using multiple regression, it is significantly predictive (P=.003) while length is not (P=.144). Therefore, treatment condition and not reduced size primarily accounts for impaired XGF social behavior.

To execute normal social orienting behavior, larval zebrafish must be able to visually detect a conspecific social stimulus and rapidly change body position to reciprocate movements of the other fish. It is possible that the microbiota influences circuitry that establishes early vision and locomotion circuitry required for social behavior to develop correctly. To simultaneously assay vision and locomotion, we compared kinetics of the optomotor response to virtual motion in 7 dpf GF larvae and

CVZ controls. We presented larvae with a full-field optomotor stimulus composed of concentric rings simulating motion toward the center of the dish.[41] This stimulus induces fish to swim toward the dish center, followed by dispersal toward the edge after the stimulus ceases (Figure 1g). We observe no significant differences in the kinetics or magnitude of responses to optomotor stimulus in GF fish relative to their CVZ siblings, suggesting that the microbiota does not influence early development of vision or motor output (Figure 1h, i). Average swim speed remains normal in 14 dpf XGF larvae relative to CVZ controls (Figure supplement 1c), suggesting that the microbiota influences circuits specific to social behavior.

The microbiota restrains vTel^{y321} neuronal arborization. We hypothesized that the microbiota could influence social behavior by influencing connectivity of vTel^{y321} neurons, which are required for normal social behavior.[3] To test this possibility, we visualized individual vTel^{y321} arbors using a sparse mosaic labeling technique, bloSwitch, that inefficiently recombines UAS-driven fluorescent proteins to generate random sparse labeling of Gal4-defined cells.[42] We used a semi-automated segmentation approach to image, reconstruct and quantify mosaic RFP-expressing vTel^{y321} neurons and the GFP-expressing reference population from CVZ and GF siblings in 3D (Figure 2a). As vTel^{y321} neurons are required for normal social behavior, we first hypothesized that the microbiota might promote social behavior by modulating the number of vTel^{y321} cells. The vTel^{y321} nucleus comprises an average of 229 neurons in 7 dpf CVZ larvae, which is slightly but statistically significantly reduced in GF larvae. However, 14 dpf XGF larvae that cannot execute normal social behavior have a similar number of vTel^{y321} neurons as their CVZ siblings, indicating that the microbiota does not influence *y321Et* promoter expression or modulate social behavior by promoting vTel^{y321} proliferation (Figure 2b).

Randomly sampling vTel^{y321} neurons across dozens of 7 dpf larval brains, we observed surprisingly diverse morphologies from short neurites with only a few branches to complex arbors hundreds of microns long (Figure 2a; CVZ: n = 73 neurons from 24 larvae; GF: n = 70 neurons from 25 larvae). Though we occasionally observed vTel^{y321} neurites projecting into adjacent brain regions including the preoptic area and hypothalamus, fasciculation of these neurites in large tracts made reconstruction of

individual arbors impossible and excluded them from analysis. The total length of vTel^{y321} arbors is significantly increased in GF larvae compared to CVZ siblings and the average length of vTel^{y321} branches remains indistinguishable, suggesting that the microbiota restrains vTel^{y321} arbor length by

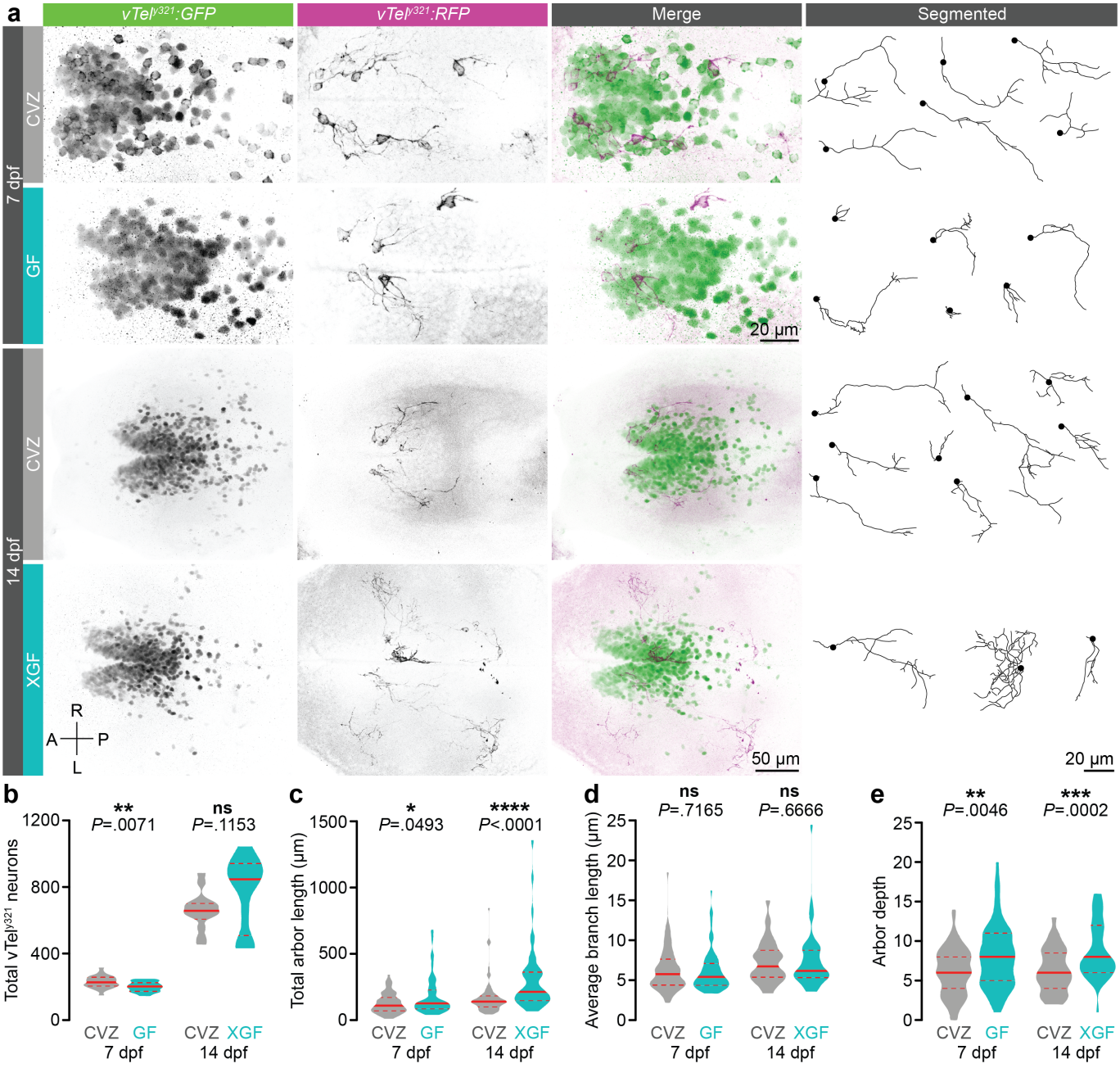

Fig. 2 The microbiota restrains vTel^{y321} arborization. **a** Maximum-intensity projections of vTel^{y321} GFP (green), sparse mosaic vTel^{y321} RFP (magenta), and individually segmented vTel^{y321} neurons from representative 7 dpf (top) or 14 dpf (bottom) larvae raised CVZ (gray), GF (aqua), or XGF (aqua). **b** The total number of vTel^{y321} GFP neurons is reduced in 7 dpf GF larvae relative to CVZ controls (n = 24 CVZ and 22 GF larvae; Unpaired t-test), but not in 14 dpf XGF larvae relative to CVZ controls (n = 14 CVZ and 12 XGF larvae; Mann-Whitney U test). **c-e** Total arbor length (**c**) and arbor depth (**e**) are increased and average branch length is unchanged (**d**) in 7 dpf GF larvae relative to CVZ controls (n = 73 neurons from 24 CVZ larvae and 69 neurons from 25 GF larvae; Mann-Whitney U tests) and in 14 dpf XGF larvae relative to CVZ controls (n = 69 neurons from 14 CVZ larvae and 46 neurons from 13 XGF larvae; Mann-Whitney U tests). ns, not significant; *, P<.05; **, P<.01; ***, P<.001; ****, P<.0001. Solid red line represents the median, dotted red lines represent the upper and lower quartiles.

modulating branching rather than outgrowth of individual neurites (Figure 2c, d). To assess this possibility, we quantified arbor depth, a measure of branching complexity corresponding to the maximum number of bifurcations on a given arbor. GF vTel^{y321} arbors are significantly deeper than those of CVZ controls, reinforcing the idea that the normal role of the microbiota is to restrain vTel^{y321} neurite branching (Figure 2c, d).

To examine whether impaired early vTel^{y321} neurite development persists in later larval stages that can execute social behavior, we reconstructed and quantified vTel^{y321} arbors in 14 dpf XGF larvae (Figure 1a, 2a; CVZ: n = 69 neurons from 14 larvae, XGF: n = 46 neurons from 13 larvae). Relative to CVZ siblings, vTel^{y321} arbors from 14 dpf XGF larvae retain the similar average branch length and increased total arbor length and depth observed in 7 dpf larvae (Figure 2c-e). Since impaired arborization in 7 dpf GF larvae persists to late larval stages of XGF fish that exhibit impaired social behavior, we conclude that early microbial modulation of neurodevelopment is critical for normal connectivity in circuits required for later expression of social behavior.

The microbiota guides vTel^{y321} arbor targeting. To assess the spatial organization of vTel^{y321} arbor complexity, we applied 3D Sholl analysis to segmented vTel^{y321} arbors in GF, XGF, and CVZ larvae. Sholl analysis quantifies the number of times each neuronal arbor intersects a series of concentric spheres, or connective zone, centered around the soma and increasing in diameter by 1 μm (insets, Figure 3a, b).[43] vTel^{y321} arbors from 7 dpf CVZ larvae cover a connective zone over 100 μm from the soma, and though arbors from GF larvae cover a similar connective zone, they exhibit a dramatic increase in complexity 10-80 μm from the soma (Figure 3a). The total number of Sholl intersections and maximum number of Sholl intersections are not dramatically different in GF larvae relative to CVZ controls, however a significant increase in both the maximum Sholl radius and Sholl radius that contains the most intersections suggests that the microbiota normally restrains distal arbor complexity (Figure 3c-f).

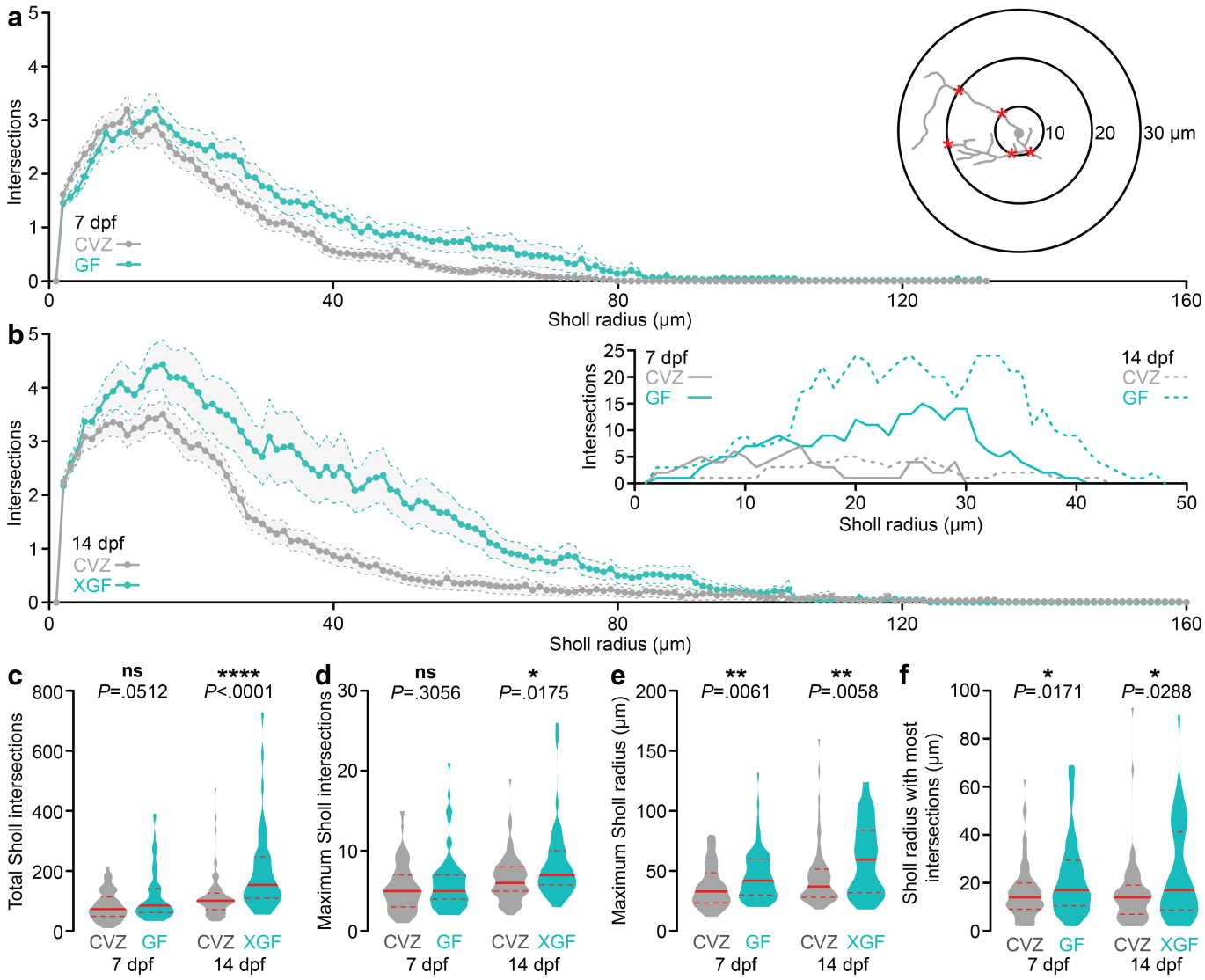

Fig. 3 The microbiota reorganizes vTel^{y321} neurite complexity. **a** Average Sholl profiles (inset) for vTel^{y321} neurons from 7 dpf larvae raised CVZ (gray) or GF (aqua). **b** Average Sholl profiles from 14 dpf larvae raised CVZ (gray) or XGF (aqua), and representative examples (inset). **c-e** Total Sholl intersections across each arbor (**c**) and maximum Sholl intersections at any radius (**d**) are not different between vTel^{y321} neurons in 7 dpf CVZ and GF larvae, but are increased in vTel^{y321} neurons in 14 dpf XGF larvae relative to CVZ siblings, whereas maximum Sholl radius (**e**) and Sholl radius with the most intersections (**f**) are increased in vTel^{y321} neurons between 7 dpf CVZ and GF larvae and between 14 dpf CVZ and XGF larvae (7 dpf, $n = 73$ neurons from 24 CVZ larvae, 69 neurons from 25 GF larvae; 14 dpf, $n = 69$ neurons from 14 CVZ larvae, 46 neurons from 13 XGF larvae; Mann-Whitney U tests). ns, not significant; *, $P<.05$; **, $P<.01$; ****, $P<.0001$. Solid red line represents the median, dotted red lines represent the upper and lower quartiles.

As with the measures of arbor complexity described above, an additional week of development following inoculation with a normal microbiota does not restore normal Sholl profiles to XGF vTel^{y321} arbors; in fact, the rearrangement observed at 7 dpf is exaggerated. Though 14 dpf CVZ vTel^{y321} arbors can cover a volume up to 160 μm from the soma, XGF vTel^{y321} arbors are nearly twice as complex as those from CVZ controls across the majority of this connective zone (Figure 3b). Total Sholl intersections, maximum Sholl intersections, maximum Sholl radius, and the Sholl radius containing the

most intersections are all significantly increased in 14 dpf XGF vTel^{y321} arbors relative to those from CVZ siblings. Therefore, early microbial modulation of vTel^{y321} arborization restrains a connective zone that continues to develop as social behavior coalesces.

The hundreds of neurons that comprise the vTel^{y321} nucleus likely include multiple morphological subtypes. We hypothesized that the microbiota might be required for normal development of specific vTel^{y321} neuronal subtypes. To address this possibility, we extracted 13 morphological parameters from segmented vTel^{y321} neurons and used hierarchical clustering (Figure 4a, c) and factor analysis (Figure 4b, d) to group them according to morphology. Factor analysis reduced the measured dimensions into three factors that explain the most variance and plotting each neuron according to its score for the first and second factors reveals morphological clusters (Figure 4b, d). Two general categories of vTel^{y321} neurons are apparent at 7 dpf: the vast majority that have simple arbors with few, short branches (Figure 4a, b: grey, aqua) and a smaller subset that have long neurites with complex branching patterns (Figure 4a, b: orange, purple). Neurons in these broad classes are further subdivided into smaller morphological clusters. vTel^{y321} neurons from GF larvae are overrepresented in clusters defined by increased morphological complexity, located on the right side of the dendrogram and factor analysis plots (Figure 4a, b). We also grouped vTel^{y321} neurons using NBLAST hierarchical clustering methods applied to zebrafish forebrain neurons in a previous study, which yielded similar results (data not shown).[44,45] Complex arbors remain over-represented in 14 dpf XGF larvae relative to their CVZ siblings (Figure 4c, d: aqua, purple). Therefore, it appears that the majority of vTel^{y321} neurons analyzed in GF or XGF fish are morphologically similar to those from CVZ siblings, but that the microbiota normally restrains arborization of a subset of vTel^{y321} neurons that become dramatically more complex in GF or XGF conditions.

To assess how the microbiota rearranges vTel^{y321} neurites relative to the rest of the forebrain, we adapted existing tools and applied an automatic, signal-based pipeline to register individual vTel^{y321} neurons to a reference vTel^{y321} nucleus (Figure 5, Supplemental movies 3-6). We expected that vTel^{y321} subtypes might express some degree of spatial arrangement according to arbor morphology, perhaps

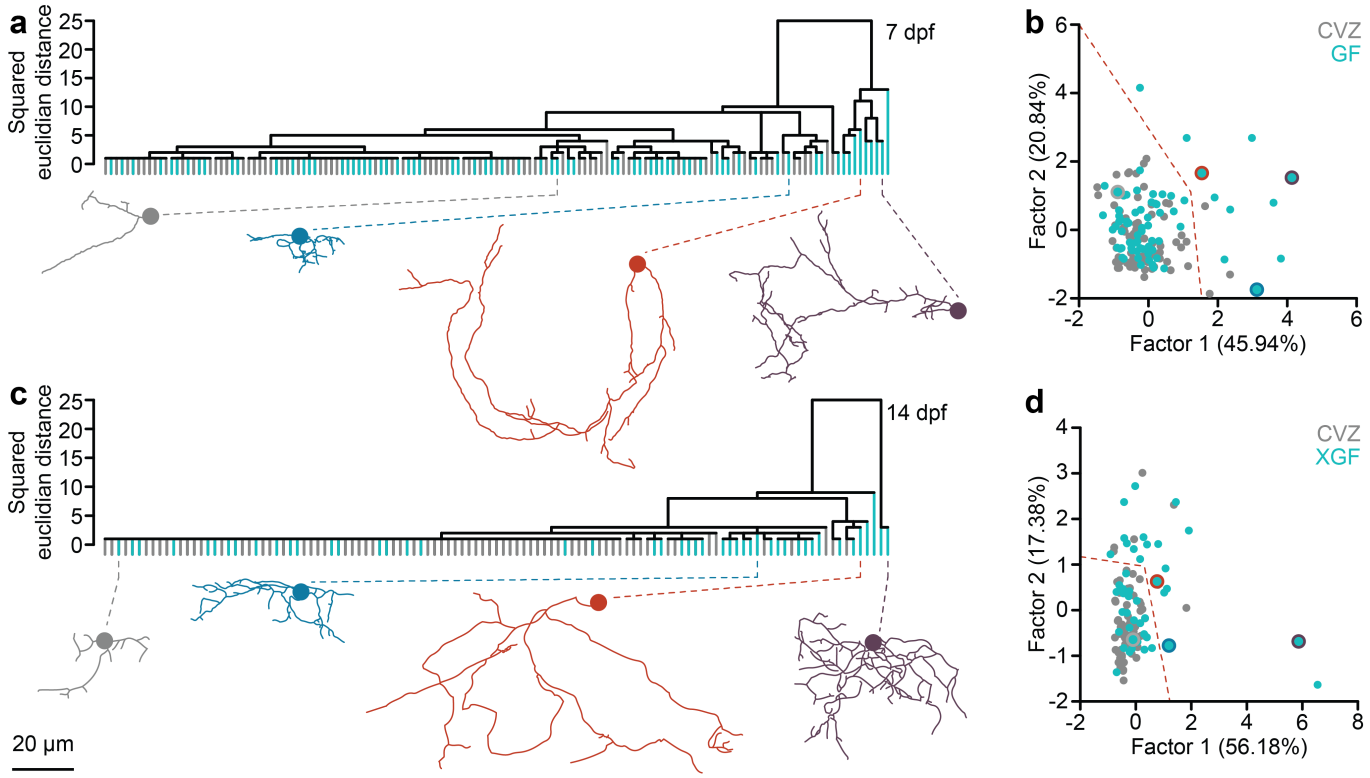

Fig. 4 The microbiota modulates a subset of vTel^{y321} arbors. **a-d** vTel^{y321} neurons from 7 dpf (**a, b**) larvae raised GF (aqua) or CVZ (gray) or 14 dpf (**c, d**) larvae raised XGF (aqua) or CVZ (gray), grouped by average linkage in hierarchical clustering (**a, c**) or by factor analysis (**b, d;** 7 dpf, $n = 73$ neurons from 24 CVZ larvae, 69 neurons from 25 GF larvae; 14 dpf, $n = 69$ neurons from 14 CVZ larvae, 46 neurons from 13 XGF larvae). Representative examples are illustrated below each dendrogram and by color in factor analysis plots. Dotted orange lines in **b** and **d** delineate two morphological classes emphasized in Figure 5.

with simple neuron somata clustered near the midline and complex neuron somata arranged at the periphery to project their neurites into adjacent functional regions. However, vTel^{y321} somata do not appear organized in obvious patterns based on neurite morphology. As expected, the most complex vTel^{y321} subtypes (orange) project their neurites predominantly into neuropil regions surrounding the vTel^{y321} nucleus and simple vTel^{y321} arbors often remain within the vTel^{y321} nucleus. At both 7 dpf (Figure 5a, Supplemental movies 3 and 4) and 14 dpf (Figure 5b, Supplemental movies 5 and 6), vTel^{y321} neurites are significantly less dense in CVZ controls than in larvae raised GF or XGF, respectively. Additionally, a lateral view (bottom panels in Figure 5a, b) reveals that the microbiota is required for vTel^{y321} neurites to reach their normal targets in the ventral portion of the anterior commissure rather than the dorsal anterior commissure targeting observed in both GF and XGF larvae.

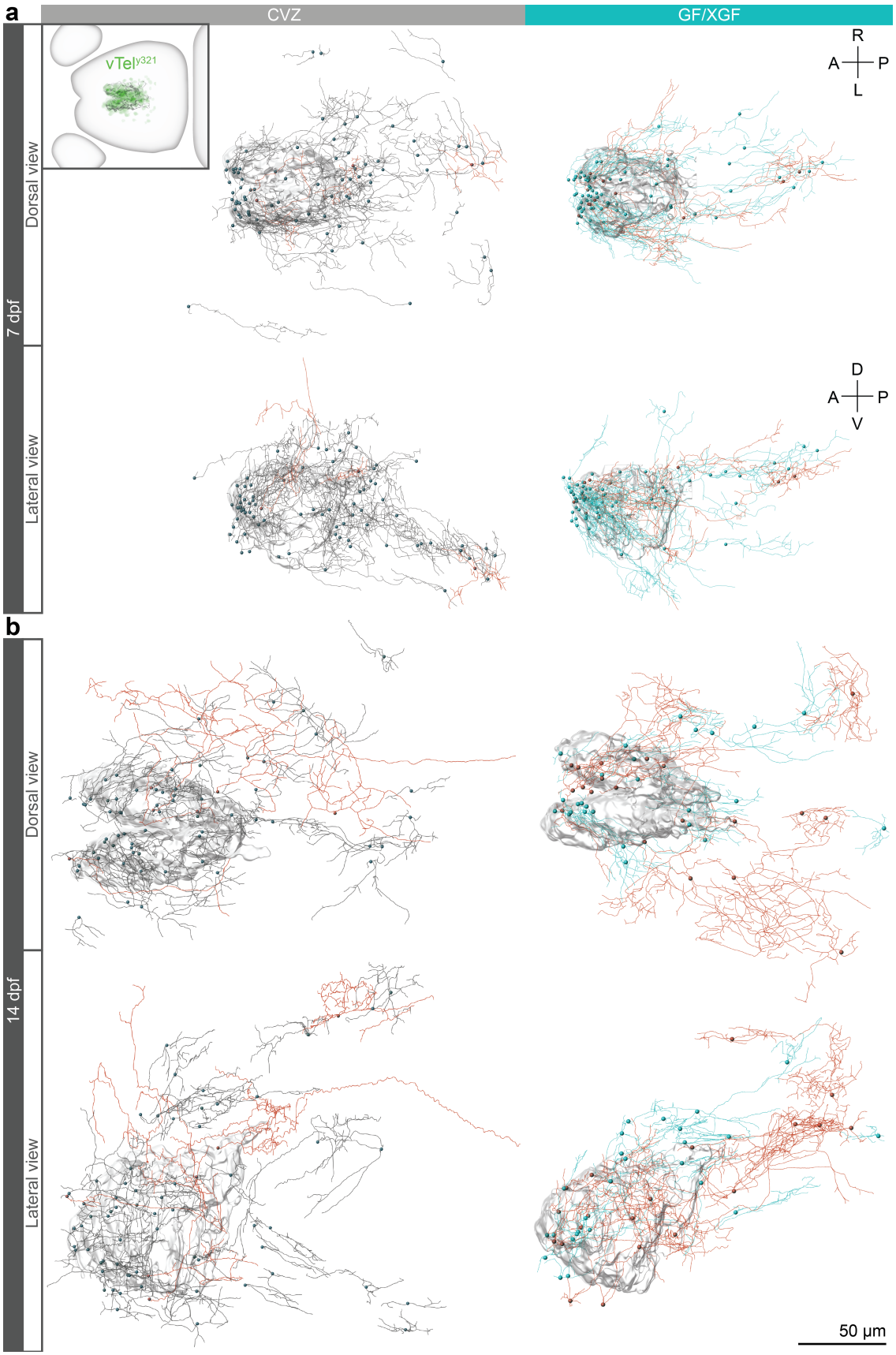
a
CVZ
GF/XGF
vTel^{y321}
R
A
P
L
D
A
P
V
7 dpf
Dorsal view
Lateral view
b
14 dpf
Dorsal view
Lateral view
50 µm

Fig. 5 The microbiota refines vTel^{y321} targeting. Dorsal (top) and lateral (bottom) views of vTel^{y321} neurons from **a** 7 dpf CVZ (gray) and GF (aqua) larvae and **b** 14 dpf CVZ (gray) and XGF (aqua) larvae registered to an average vTel^{y321} nucleus (transparent 3D model) from each condition and developmental stage. Average vTel^{y321} nuclei do not incorporate sparse neuronal somata at the periphery, which are within the forebrain boundary. Neurons right of the dotted line in the factor analysis plots in Figure 4b and d are indicated in orange.

The microbiota promotes forebrain microglia abundance. We hypothesized that the microbiota might restrain vTel^{y321} arborization via microglia, the brain's resident immune cells that regulate neurite outgrowth and pruning.[29] Though social phenotypes are not expressed until 14 dpf, our experiments provide evidence that the microbiota modulates vTel^{y321} neuronal morphology by 7 dpf. If the microbiota exerts this influence by modulating development of forebrain microglial populations, then altered microglia should be apparent in 7 dpf GF larvae. To test this hypothesis, we compared forebrain microglia of GF *mpeg1:mCherryTg* larvae to those of CVZ sibling controls (Figure 6a). The total number of *mpeg1:mCherryTg*-positive cells in the rostral portion of the head is significantly reduced in GF larvae compared to CVZ controls (Figure 6b).The *mpeg:mCherry* transgene is expressed in both microglia and circulating macrophages, so we then used brightfield images to segment the CNS boundary and distinguish these cell types. Initial microglial accumulation in the zebrafish CNS largely occurs before microbiota colonization, so developmental delay between GF and CVZ larvae should not affect microglial establishment in the brain.[36,46] However, since microglia distribution remains dynamic after colonization and some GF larvae are slightly smaller than their CVZ siblings, microglial counts were normalized to forebrain axial length. The subpopulation of microglia embedded in the GFP-labelled vTel^{y321} nucleus is significantly reduced in GF larvae relative to CVZ controls, reinforcing the conclusion that the microbiota is required for normal microglial abundance in the zebrafish forebrain (Figure 6c).

The microbiota does not influence forebrain microglial morphology or activity. It is possible that in addition to promoting microglial development or infiltration, the microbiota also promotes microglial phagocytic activity, which is required for their role in responding to local insult, clearing apoptotic material, and for normal synaptic pruning and maturation during brain development.[47,48] Microglia executing these activities have distinct morphologies, which consequently can be used to assay

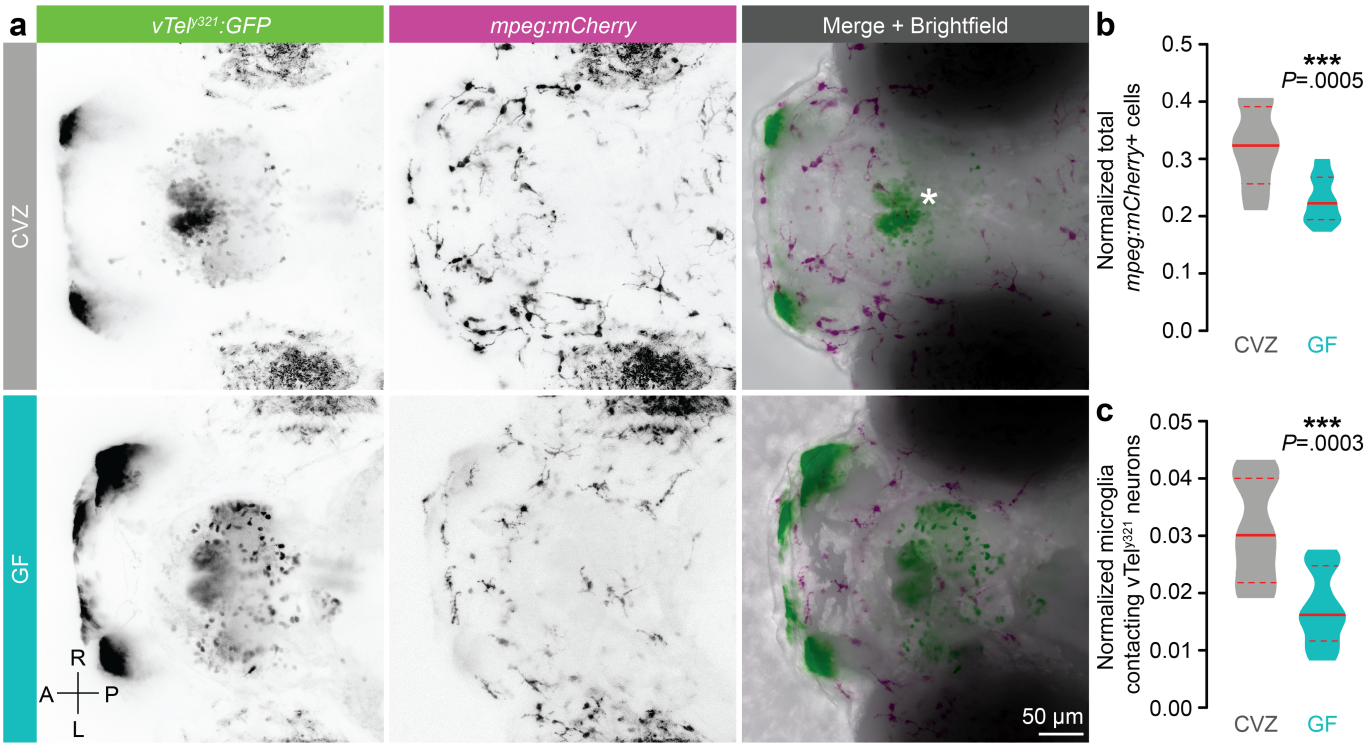

Fig. 6 The microbiota promotes forebrain microglial infiltration. **a** Dorsal views of maximum-intensity projections of vTel^{y321} GFP (neurons, green) and *mpeg1:mCherryTg* (microglia and macrophages, magenta) in CVZ (gray) and GF (aqua) 7 dpf larval heads. Both **b** total *mpeg1:mCherryTg*-positive cells and **c** the subset of *mpeg1:mCherryTg*-positive cells embedded in the forebrain and contacting vTel^{y321} neurites are reduced in GF larvae relative to CVZ siblings (n = 8 CVZ and 17 GF larvae; Unpaired t-test). ***, P<.001. Solid red line represents the median, dotted red lines represent the upper and lower quartiles.

microglial activity. Microglia are traditionally classified as either “ramified” or “amoeboid;” ramified microglia do not travel through the tissue but scan relatively stable territory with dynamic processes that monitor, maintain, and prune synapses.[47–49] Amoeboid microglia retract many of their processes and can proliferate and migrate through the tissue in response to molecular or physical challenge. To test whether the microbiota influences neurodevelopment by affecting microglial morphology in the forebrain, we used semi-automated fluorescence-based segmentation of 20-minute spinning-disk confocal volumetric time series to quantify *mpeg1:mCherryTg*-positive microglia embedded in the vTel^{y321} nucleus (Figure 7a). In 7 dpf GF larvae and CVZ controls, we observe diverse morphologies that include ramified microglia with long, complex branching patterns and amoeboid microglia with larger cell bodies and fewer branches (Figure 6). Across the time series, we do not observe significant differences in microglial morphology (Figure 7b, c) or kinetics (Figure 7d, e, Supplemental movies 7 and 8) in GF and CVZ larvae.

Though this suggests that the microbiota does not influence forebrain microglial dynamics, assessing morphological variance at the single-cell level may underestimate the motility of microglial processes. To address this possibility, we estimated spatial sampling of forebrain microglial protrusions by

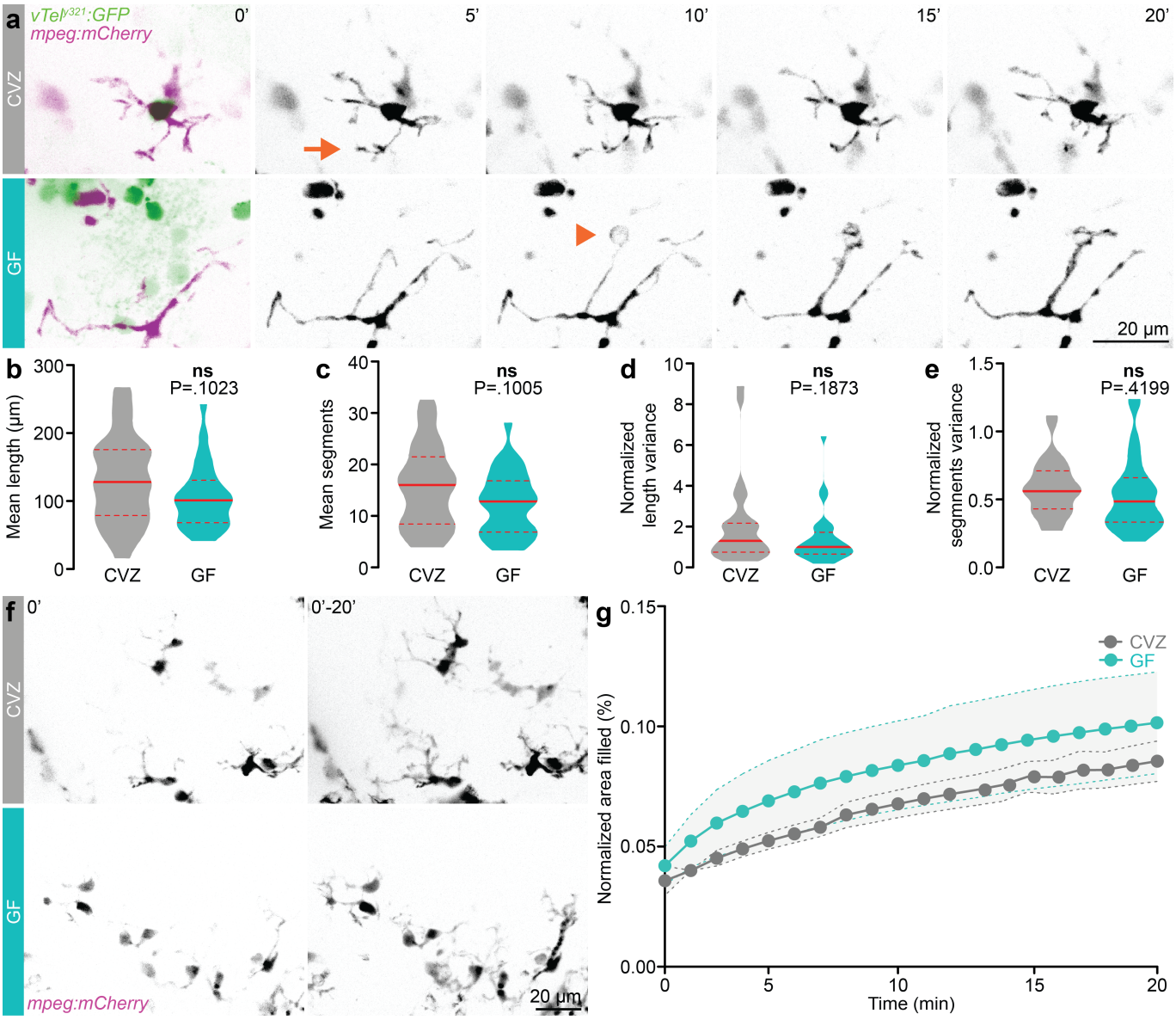

Fig. 7 The microbiota does not influence forebrain microglial activity. **a** Maximum-intensity Z-projections of representative *mpeg1:mCherryTg*-positive microglia (magenta) and vTel^{y321} neurons (green), from CVZ (gray) and GF (aqua) larvae, every five minutes across a 20-minute time series. Arrow indicates a rapidly retracting protrusion and arrowhead indicates an extending protrusion that likely envelops an unlabeled neuronal soma. **b** mean length, **c** mean number of segments, **d** mean-normalized length variance, and **e** mean-normalized segments variance of vTel^{y321}-embedded microglia across the time series are similar in GF larvae and CVZ siblings (n = 28 microglia from 4 CVZ larvae and 28 microglia from 3 GF larvae; Unpaired t-test for mean length, mean segments, and mean-normalized segments variance; Mann-Whitney U test for mean-normalized length variance). **f** Maximum-intensity Z projections of *mpeg1:mCherryTg*-positive microglia from representative CVZ (gray, top) and GF (aqua, bottom) larvae in the first frame (0') of a 20-minute spinning disc confocal time series and after cumulative intensity projection across the time series (0'-20'). **g** Volume-normalized fraction of the forebrain filled by *mpeg1:mCherryTg* signal in cumulative projections of 20-minute time series of CVZ (gray) and GF (aqua) larval forebrains (n = 4 CVZ and 3 GF larvae). Solid lines represent the mean, dotted lines represent SEM. ns, not significant. Solid red line represents the median, dotted red lines represent the upper and lower quartiles.

quantifying the fraction of the segmented area filled by vTel^{y321}-resident microglia in cumulative maximum-intensity projections through each 20-minute time series, normalizing each measurement by the z-volume of each z-projected time series (Figure 7f).[47] Over 20-minutes of activity, microglia in GF larvae do not survey a greater percentage of the forebrain than microglia in CVZ controls (Figure 7g). Therefore, two measures of microglial dynamics suggest that the microbiota does not influence forebrain microglial activity and that microglial activity does not increase to compensate for the reduced number of microglia in GF larvae. These results are consistent with our hypothesis that the increased arborization of GF vTel^{y321} neurons results from decreased pruning due to a paucity of vTel^{y321}-resident microglia.

Discussion

The key finding of our study is that the microbiota is required during an early period of development for zebrafish to develop normal social behavior that only manifests at a later developmental stage (Figure 8). This behavior requires the vTel ^{y321} nucleus, which is homologous to 'social nuclei' in other vertebrate models. We found that the microbiota significantly alters projections of a subset of vTel ^{y321} neurons by restraining neurite complexity. We also found that the microbiota is required for infiltration of the appropriate number of microglia into the vTel ^{y321} brain region, raising the possibility that microbial modulation of neurite complexity depends on the size of the microglial population available to refine vTel^{y321} neurites. We discuss each of these points in turn.

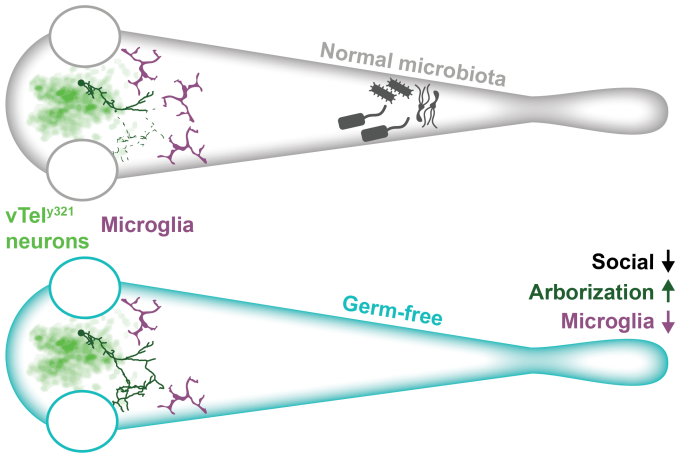

Fig. 8 The microbiota promotes zebrafish social behavior, retargets vTel^{y321} connectivity by restraining neurite complexity, and promotes forebrain microglial infiltration without influencing microglial activity.

We observed that the microbiota is required early for normal social behavior exhibited at least a week later, suggesting that the microbiota influences social behavior by modulating neurodevelopment during an early sensitive period. The microbiota has been linked to preference for social novelty in mice, but it was unclear whether the microbiota was required for normal social interaction in any vertebrate.[16,18] A previous study identified an *L. rhamnosus* strain that can promote shoaling in otherwise conventionally-raised zebrafish, but ours is the first study to demonstrate that an intact microbiota is required for normal zebrafish social behavior such as conspecific orienting (Figure 1).[24] The zebrafish microbiota is also required for normal activity and anxiety-like behavior, suggesting that these phenotypes could be linked to the impaired social behavior we observe.[26] However, GF larvae and their CVZ siblings perform similarly in our optomotor assay and motor behavior remains unaffected in 14 dpf XGF larvae, so the social defects we observe in XGF larvae are likely independent of an effect on activity and may result from impaired integrative circuits downstream of sensory input and upstream of motor output (Figure 1, Figure Supplement 1). Altered anxiety-like behavior has also been reported in GF mice, so future experiments could explore whether microbial modulation of anxiety and social behavior intersect in brain regions like the subpallium, which in zebrafish includes vTel^{y321} neurons.[50] Further studies are also necessary to parse the host-associated microbiota and identify specific microbial species or products that are required for normal neurodevelopment and social behavior.

As the microbiota is required early for later-developing social behavior, we postulated that it influences early neurodevelopmental events specifically in circuits that regulate social behavior. Therefore, we focused on whether the microbiota is required for normal development of subpallial vTel^{y321} neurons, which are required for normal social behavior.[3] Though analogy between teleost fish and mammals is complicated by differences in embryonic neural tube formation, developmental, neurochemical, and hodological similarities suggest that the zebrafish vTel is part of a social behavior circuit with homologs in mammalian brain regions including the lateral septum, preoptic area, and hypothalamus.[10–12] Whether development of these regions, which regulate social behavior in mice, is also influenced by microbial signals has not been investigated. However, several previous studies found that the

microbiota is required for normal dendrite morphology in the murine anterior cingulate cortex, amygdala, and hippocampus, so it seems likely that microbial modulation of social behavior in other vertebrates could also occur by modulation of circuit connectivity as we observed in zebrafish vTel^{y321} neurons.[51,52] These changes in neuronal morphology could be, at least in part, a downstream effect of microbial modulation of gene expression. Though studies examining the microbial modulation of neuronal gene expression have largely focused on cortex and the hippocampus, altered amygdala expression of genes including *BDNF* and multiple neurotransmitter pathways could also affect social behavior by modifying neuronal morphology or connectivity.[16,22,50,53–55] For example, oxytocin signaling in the murine hypothalamus is altered following probiotic treatment.[56–58] As the hypothalamus is a vTel^{y321} analog and oxytocin signaling is important for zebrafish social behavior, it will be interesting to investigate whether microbial modulation of social behavior, neuronal gene expression, and cytoarchitecture intersect in forebrain neuromodulatory systems.[59]

Neuronal morphology is the foundation for circuit connectivity and function, so our finding that the microbiota influences the morphology and targeting of subpallial vTel^{y321} neurons provides strong evidence that the microbiota normally plays a critical role in establishing social circuitry. The exuberant arborization we observe early in GF fish persists even with an additional week of development in the presence of normal microbes (Figures 2-5), suggesting that vTel^{y321} connectivity impaired during early development results in persistently miswired circuits. Microbial modulation of neurite complexity appears critical for normal ventral targeting many vTel^{Y321} neurites; we observed GF or XGF vTel^{y321} neurites reaching dorsal destinations not apparent in CVZ controls (Figure 5). It will be interesting to further investigate the functional consequences of vTel^{y321} neurite ventral targeting. Significant dopaminergic neurons and projections populate the most ventral aspects of the zebrafish subpallium and could synapse with vTel^{y321} neurites that project ventroposteriorly toward the anterior commissure, raising the exciting possibility that vTel^{y321} neurons interact directly with monoamine circuits known to regulate social reward.[60–63]

We have shown that the microbiota is critical for normal vTel^{y321} neuronal morphology. However, it is unclear whether all of the neurite defects we observe in GF and XGF larvae represent failure of arbor refinement or whether there is also exuberant initial outgrowth. Since microglia are ideally positioned to both receive microbial signals and modify neurons, we hypothesized that the microbiota promotes social behavior by influencing development or function of microglia that modify vTel^{y321} neurites. There is precedence for this idea in the literature – antibiotic-induced dysbiosis in mice impairs their response to social novelty and induces morphologically "active" microglia in the hippocampus and cortex.[54] Microglia in GF mice are also larger, less mature, less responsive to LPS challenge, and more abundant in the cortex, corpus callosum, hippocampus, olfactory bulb, and cerebellum than in specific pathogen free (SPF) controls.[64] Contrary to these phenotypes, the microglial subpopulation directly embedded in the vTel^{y321} nucleus is reduced in GF larvae relative to CVZ controls (Figure 6), and vTel^{y321} microglial morphology or dynamics, which correlate with pruning and phagocytic activity, do not appear influenced by the microbiota (Figure 7). How can these results be reconciled? One possibility is that the microbiota has differential effects on microglia across the brain. Microglia are drawn into the brain by chemokine signaling and neuronal apoptosis before 4 dpf, prior to microbiota colonization.[36,46,65] The number of vTel^{y321} neurons is similar in GF and CVZ fish, and apoptotic neurons are largely absent by 6 dpf, so it is unlikely that the microbiota draws microglia to the developing forebrain by promoting apoptosis.[46] It therefore seems likely that in GF larvae either a "microglial persistence" signal is missing from the vTel^{y321}, microglia are drawn out of the vTel^{y321} by a chemoattractant elsewhere in the brain, or that local microglial proliferation is affected. It is also possible that the microbiota has differential effects on early larval and juvenile microglia, which have distinct developmental origins and neuro-immune functions.[33] Further study will be necessary to gain a deeper understanding of the role of the microbiota in promoting or suppressing microglial development or dynamics and how this varies across brain regions and developmental time.

Effective intervention in diverse neurodevelopmental disorders requires understanding both intrinsic and extrinsic pathways that guide development. The neurodevelopmental processes that build social

behavior across taxa are poorly understood. Our study reveals microbial modulation of social behavior in a model vertebrate well-suited to simultaneous study of the microbiota, brain and immune system, and provides a first in-depth look at how interactions among these components modulate circuit formation and maintenance. Future studies will further understanding of host functions and the microbial molecular inputs that modulate their development.

Materials and Methods

Ethics statement. All zebrafish experiments were approved by the University of Oregon Institutional Animal Care and Use Committee (protocols 18-08 and 18-29).

Zebrafish lines and husbandry. All zebrafish lines were maintained as previously described at 28° C with a 14/10 light/dark cycle.[66] AB x TU strain wild-type fish were raised CVZ and GF for behavior experiments. For vTel^{y321} sparse mosaic labelling, *Tg(14xUAS-E1b:UBCi-blo-nls-emGFP-βglobin-blo-lyn-TagRFPT-afp)y562* (*UAS:bloSwitch*) and *Tg(myl7:GFP-hsp70l:B3r-2a-Cer)y560* (*hsp70l:B3*) lines gifted by the Burgess laboratory were crossed to *Et(REX2-SCP1:GAL4FF)y321* (*y321Et)* by maintaining a stable line heterozygous for *UAS:bloSwitch* and *y321Et* which was then crossed to *hsp70l:B3*.[42] For simultaneous imaging of microglia and vTel^{y321} neurons, homozygous *y321Et; UAS:GFP* fish were crossed to homozygous *Tg(mpeg1:mCherry)^{gl23}* (*mpeg1:mCherryTg*). AB x TU, *y321Et*, *UAS:GFP*, and *mpeg1:mCherryTg* lines are available from the Zebrafish International Resource Center (ZIRC; http://zebrafish.org).

Gnotobiology. Zebrafish embryos were raised GF, XGF, or CVZ as previously described.[39,67] Briefly, embryos were treated from 0-6 hours post-fertilization (hpf) in embryo medium (EM) containing 100 μg/mL ampicillin, 250 ng/mL amphotericin B, 10 μg/mL gentamycin, 1 μg/mL tetracycline, and 1 μg/mL chloramphenicol. In a class II A2 biological safety cabinet, embryos were briefly surface-sterilized with 0.1% PVP-I and 0.003% sodium hypochlorite, washed with sterile EM, and transferred to 50 mL tissue culture flasks at a density of 1 fish/1 mL sterile EM. CVZ flasks were inoculated with 200 μl water from the parental tank. Sterility was assessed by direct visualization of microbial contaminants with phase

optics on an inverted microscope at 40x magnification once per day and by culturing media on LB agar at 28° C for two days following terminal sampling. XGF larvae and CVZ siblings were inoculated with system water at 7 dpf and fed rotifers three times daily until terminal sampling at 14 dpf.

Behavior. Social behavior was assessed with our previously published dyad assay for post-flexion larval and adult zebrafish.[2,3] Briefly, AB x TU 14 dpf sibling pairs for each condition were placed in isolated custom-built acrylic tanks (50 mm width x 50 mm length x 20 mm depth), and allowed to interact for 10 minutes via adjoining transparent tank walls. Larvae were imaged from below at 10 fps using a Mightex SME-B050-U camera. The arena was illuminated from above with a white LED panel (Environmental Lights) with light-diffusing plastic as a tank lid to improve image quality. Fish that spent <10% of the experiment in motion (moving at least one-third of their total body length per frame) were not included in subsequent analysis. Social interaction was defined as the average relative distance from the divider and the percentage of time spent orienting at 45°–90°, and these parameters were measured and analyzed using our previously described computer vision software written in Python (available at https://github.com/stednitzs/daniopen). To account for changes in nutrition between fish, standard length was measured as previously described.[40]

Optomotor response was assessed using a previously described "virtual reality" system for assessing zebrafish behavior, measuring swim response in 7 dpf larvae to concentric rings simulating motion towards the center of a dish.[68] Briefly, we used infrared illumination to simultaneously record the swim responses of 9 AB x TU larvae at a time in 10 cm shallow glass dishes filled with EM. Larvae were imaged at 30 frames per second. Visual stimulus was projected on a screen underneath the dishes for 20 seconds and consisted of concentric rings moving toward the dish center, followed by a 20-second refractory period. Responses are the average of 46-59 stimulus trials per fish, presented over 1-hour.

Sparse mosaic neuronal labeling. For sparse mosaic recombination of GFP and RFP transgenes in vTel^{y321} neurons, *y321Et; UAS-bloswitch; hsp70lB3* larvae were heat shocked 24 hours ahead of

terminal sampling (at 6 dpf or 13 dpf) by immersing sterile flasks in a 37 ^{o} C water bath for 30 minutes. Larvae were returned to 28° C for an additional day following heat shock.

Immunocytochemistry. Larval zebrafish were immunolabeled as previously described.[3] Briefly, 7 dpf larvae were euthanized with MS-222, fixed in 4% paraformaldehyde at room temperature overnight, permeabilized in phosphate-buffered saline (PBS) with 0.5% Triton X-100, and then blocked overnight at room temperature in PBS with 0.5% Triton X-100, 5% normal goat serum, 2% bovine serum albumin, and 1% DMSO. Larvae were then treated with primary antibodies overnight at room temperature diluted in blocking solution at the concentrations indicated below, washed, and treated with secondary antibodies diluted 1:1000 in PBS with 0.5% Triton X-100 for 6 hours at room temperature. Finally, larvae were washed in PBS with 0.5% Triton X-100, eyes, lower jaws, and tails were removed, and the remaining tissue was mounted in Prolong Diamond anti-fade mountant (Invitrogen Cat# P36970). At 14 dpf, larvae were euthanized on ice and pre-fixed in 4% paraformaldehyde for 1 hour. The midbrain and forebrain was dissected in PBS, removed, and fixed overnight at room temperature in 4% paraformaldehyde. We used a modified CUBIC protocol for clearing and immunolabeling dissected 14 dpf larval brains.[69] Brains were rinsed in PBS and incubated in CUBIC 1 solution (25% wt urea, 25% wt Quadrol, and 15% wt Triton X-100 in dH_2O) at 37 ^{o} C for 2-3 days. Brains were then washed, blocked, and incubated with primary antibodies as described above. After additional washing steps, brains were incubated with secondary antibodies diluted 1:100 in PBS with 0.5% Triton X-100 overnight at room temperature. Brains were then briefly washed, incubated in CUBIC 2 solution (25% wt urea, 50% wt sucrose, and 10% wt triethanolamine in dH_2O) at room temperature for 6 hours, and mounted in Prolong Diamond anti-fade mountant (Invitrogen Cat# P36970). The following primary antibodies were used: mouse anti-GFP (1:100; Invitrogen Cat #A-11120) and rabbit anti-mCherry (1:100; Novus Biologicals Cat #2-25157). The following secondary antibodies were used: Alexa Fluor 488 goat anti-mouse IgG (Invitrogen Cat #A28175) and Alexa Fluor 546 goat anti-rabbit IgG (Invitrogen Cat #A-11035).

Microscopy. For quantification of neuronal morphology and microglia infiltration, fixed and immunostained larval brains were imaged on a Leica TCS SP8 X (Leica Microsystems, Wetzlar, Germany) or Zeiss LSM 880 (Carl Zeiss Microscopy, LLC, Thornwood, New York, USA) confocal microscope. Neuronal arbors were imaged with a 40x lens (1.10 NA) and microglia were imaged with a 20x lens (0.75 NA). Z stacks were acquired at 1 μm per slice through the entire forebrain. To ensure comparable resolution across samples and conditions, projections outside of a single field of view at 40x were captured by tiling multiple z stacks in Leica LAS X 3.1.5.16308 software (Leica Microsystems, Wetzlar, Germany). Microglial dynamics were imaged live in 7 dpf *y321Et; UAS:GFP; mpeg1:mCherryTg* heterozygotes raised GF or CVZ on a Nikon CSU-W1 SoRa spinning disk confocal microscope (Nikon Instruments, Inc., Melville, New York, USA) with 20x lens, imaging a z stack with 1 μm slice depth encompassing the larval forebrain every 30 or 60 seconds for 20 minutes. Time series imaged every 30 seconds were downsampled to every 60 seconds for consistency across the dataset.

Image analysis. Neuronal morphology was extracted from confocal z stacks by 3D segmentation in Imaris software (Oxford Instruments, Zurich, Switzerland) as previously described.[42] Briefly, Imaris Filament Tracer was used in “AutoPath” mode to semi-automatically segment neurites based on RFP fluorescence signal. The number of recombined cells in each brain varied from none to dozens; only arbors that could be accurately distinguished without overlap from neighboring cells were segmented. Statistics and a .swc representation were exported from each filament object for further analysis and visualization. The number of cells in the GFP-positive population was estimated by threshold-based surface creation using the “split touching objects” function and identical estimated cell size applied across all samples and conditions. Microglial morphology was quantified by semi-automatic signal-based segmentation with Imaris Filament Tracer across each time series. Cumulative intensity projections were generated in the FIJI distribution of ImageJ, manually segmented to exclude *mpeg1:mCherry* signal from circulating macrophages outside of the brain, and % area filled was measured.[70]

Image registration. Average CVZ and GF forebrains were generated separately using vTel^{y321} GFP signal as a reference. Specifically, a single brain with representative size and orientation was first chosen as a reference for each condition. Each additional brain was then registered to these templates using the Computational Morphology Toolkit (CMTK), executing the following parameters via the terminal: -awr 01 -T 4 -X 26 -C 8 -G 80 -R 4 -A '--accuracy 0.4' -W '--accuracy 0.4' -s. The resulting transformed vTel^{y321} GFP images were then averaged to generate a single average forebrain for each condition. Each original image was then registered again, this time to the condition average in CMTK with the parameters described above. This generated transformed images and image rotation, translation, scaling, shearing, and centering coordinates used to achieve that transformation. These transformation coordinates were then applied to SWC-formatted neurons using Natverse package functions in R.[45] Formatting neurons as SWC files converts them into a matrix of (x,y,z) coordinates so that they can be read across platforms. For each condition, transformed neurons were exported from R in SWC format and imported into the average vTel^{y321} GFP forebrain for 3D visualization in Imaris software (Oxford Instruments, Concord MA).

Statistics. Groups were statistically compared as described in the figure legends in Prism 8 software (Graphad, San Diego, CA, USA). Gaussian distribution of each group was examined by a D'Agostino-Pearson test of skewness and kurtosis. Unpaired t tests were applied to data with Gaussian distribution and equal standard deviation, and Welch's correction was applied if standard deviation of the two groups was unequal. Mann-Whitney *U* tests were applied to data that were not normally distributed. $P < 0.05$ was considered statistically significant. Outliers were not removed from any experimental groups. SPSS Statistics 26 (IBM, New York, USA) was used for hierarchical clustering and cluster analysis based on 13 morphological features extracted from individual neurons in Imaris. Hierarchical clustering measured the squared Euclidean distance between neurons using between-groups linkage of measurements transformed by z-scores. Underlying morphological features were extracted by principal axis factoring using a varimax rotated component matrix for variable assignments and eigenvalue cutoff

of 1. In both 7 dpf and 14 dpf datasets, three factors accounted for the majority of variance in the measurements (77.46% and 80.39% respectively).

Author Contributions. J.J.B., S.J.S, P.W., and J.S.E. designed research; J.L. and A.T. provided experimental resources; J.J.B., S.J.S, and M.G. performed research and analyzed data; J.J.B. wrote the paper; J.J.B., S.J.S, M.G., J.L., A.T., P.W., and J.S.E. edited the paper.

Acknowledgements. We thank members of the Eisen and Washbourne laboratories for feedback on earlier versions of the manuscript, members of the Guillemin laboratory and University of Oregon Microbial Ecology and Theory of Animals (META) center for gnotobology support, Adam Christensen and the University of Oregon Zebrafish Facility Staff for animal husbandry, and Harold Burgess for the generous gift of zebrafish lines. The work was supported by: Life Sciences Research Foundation Postdoctoral Fellowship and NIH F32MH118809 to J.J.B., NIH T32HD007248 and Oregon Developmental Biology Collaboration Award to S.J.S., NIH R21MH104188 and R33MH104188 to J.S.E. and P.W., and a fellowship from the John Simon Guggenheim Memorial Foundation to J.S.E.

References

1. Fernandes, J. M., Cajão, R., Lopes, R., Jerónimo, R. & Barahona-Corrêa, J. B. Social Cognition in Schizophrenia and Autism Spectrum Disorders: A Systematic Review and Meta-Analysis of Direct Comparisons. *Front. Psychiatry* **9**, 504 (2018).
2. Stednitz, S. J. & Washbourne, P. Rapid Progressive Social Development of Zebrafish. *Zebrafish* (2020) doi:10.1089/zeb.2019.1815.
3. Stednitz, S. J. *et al.* Forebrain Control of Behaviorally Driven Social Orienting in Zebrafish. *Curr. Biol.* **28**, 2445-2451.e3 (2018).
4. Dreosti, E., Lopes, G., Kampff, A. R. & Wilson, S. W. Development of social behavior in young zebrafish. *Front. Neural Circuits* **9**, 78 (2015).
5. Hinz, R. C. & Polavieja, G. G. de. Ontogeny of collective behavior reveals a simple attraction rule. *Proc. Natl. Acad. Sci.* **114**, 2295 2300 (2017).
6. Madeira, N. & Oliveira, R. F. Long-Term Social Recognition Memory in Zebrafish. *Zebrafish* **14**, 305–310 (2017).
7. Suriyampola, P. S. *et al.* Zebrafish Social Behavior in the Wild. *Zebrafish* **13**, 1–8 (2016).
8. Kyle, A. L., Stacey, N. E. & Peter, R. E. Ventral telencephalic lesions: effects on bisexual behavior, activity, and olfaction in the male goldfish. *Behav. Neural Biol.* **36**, 229–241 (1982).
9. Shinozuka, K. & Watanabe, S. Effects of telencephalic ablation on shoaling behavior in goldfish. *Physiol. & Behav.* **81**, 141–148 (2004).
10. Wullimann, M. F. & Mueller, T. Teleostean and mammalian forebrains contrasted: Evidence from genes to behavior. *J. Comp. Neurol.* **475**, 143–162 (2004).
11. O'Connell, L. A. & Hofmann, H. A. Evolution of a vertebrate social decision-making network. *Sci. (New York, NY)* **336**, 1154 1157 (2012).

12. O'Connell, L. A. & Hofmann, H. A. The Vertebrate mesolimbic reward system and social behavior network: A comparative synthesis. *J. Comp. Neurol.* **519**, 3599–3639 (2011).

13. Zhou, C. *et al.* Lhx6 and Lhx8: cell fate regulators and beyond. *FASEB J.* **29**, 4083–4091 (2015).

14. Marquart, G. D. *et al.* A 3D searchable database of transgenic zebrafish gal4 and cre lines for functional neuroanatomy studies. *Front. Neural Circuits* **9**, 1–17 (2015).

15. Sherwin, E., Bordenstein, S. R., Quinn, J. L., Dinan, T. G. & Cryan, J. F. Microbiota and the social brain. *Science (80-.).* **366**, eaar2016 (2019).

16. Arentsen, T., Raith, H., Qian, Y., Forssberg, H. & Diaz Heijtz, R. Host microbiota modulates development of social preference in mice. *Microb. Ecol. Health Dis.* **26**, 29719 (2015).

17. Arentsen, T. *et al.* The bacterial peptidoglycan-sensing molecule Pglyrp2 modulates brain development and behavior. *Mol. Psychiatry* **22**, 257–266 (2016).

18. Desbonnet, L., Clarke, G., Shanahan, F., Dinan, T. G. & Cryan, J. F. Microbiota is essential for social development in the mouse. *Mol. Psychiatry* **19**, 146–148 (2014).

19. Gacias, M. *et al.* Microbiota-driven transcriptional changes in prefrontal cortex override genetic differences in social behavior. *Elife* **5**, e13442 (2016).

20. Lu, J. *et al.* Microbiota influence the development of the brain and behaviors in C57BL/6J mice. *PLoS One* **13**, e0201829 (2018).

21. Buffington, S. A. *et al.* Microbial Reconstitution Reverses Maternal Diet-Induced Social and Synaptic Deficits in Offspring. *Cell* **165**, 1762–1775 (2016).

22. Diaz Heijtz, R. *et al.* Normal gut microbiota modulates brain development and behavior. *Proc. Natl. Acad. Sci.* **108**, 3047 3052 (2011).

23. Chen, K. *et al.* Drosophila Histone Demethylase KDM5 Regulates Social Behavior through Immune Control and Gut Microbiota Maintenance. *Cell Host Microbe* **25**, 537-552.e8 (2019).

24. Borrelli, L. *et al.* Probiotic modulation of the microbiota-gut-brain axis and behaviour in zebrafish. *Sci. Rep.* **6**, 30046 (2016).

25. Davis, D. J. *et al.* Lactobacillus plantarum attenuates anxiety-related behavior and protects against stress-induced dysbiosis in adult zebrafish. *Sci. Rep.* **6**, 33726 (2016).

26. Davis, D. J., Bryda, E. C., Gillespie, C. H. & Ericsson, A. C. Microbial modulation of behavior and stress responses in zebrafish larvae. *Behav. Brain Res.* **311**, 219–227 (2016).

27. Zhou, Z. *et al.* Identification of highly-adhesive gut Lactobacillus strains in zebrafish (Danio rerio) by partial rpoB gene sequence analysis. *Aquaculture* **370–371**, 150–157 (2013).

28. Roeselers, G. *et al.* Evidence for a core gut microbiota in the zebrafish. *ISME J.* **5**, 1595–1608 (2011).

29. Wright-Jin, E. C. & Gutmann, D. H. Microglia as Dynamic Cellular Mediators of Brain Function. *Trends Mol. Med.* **25**, 967–979 (2019).

30. Abdel-Haq, R., Schlachetzki, J. C. M., Glass, C. K. & Mazmanian, S. K. Microbiome–microglia connections via the gut–brain axis. *J. Exp. Med.* **216**, 41–59 (2019).

31. Nelson, L. H. & Lenz, K. M. Microglia depletion in early life programs persistent changes in social, mood-related, and locomotor behavior in male and female rats. *Behav. Brain Res.* **316**, 279–293 (2016).

32. Zhan, Y. *et al.* Deficient neuron-microglia signaling results in impaired functional brain connectivity and social behavior. *Nat. Neurosci.* **17**, 400–406 (2014).

33. Prinz, M., Erny, D. & Hagemeyer, N. Ontogeny and homeostasis of CNS myeloid cells. *Nat. Immunol.* **18**, 385–392 (2017).

34. Ferrero, G. *et al.* Embryonic Microglia Derive from Primitive Macrophages and Are Replaced by cmyb-Dependent Definitive Microglia in Zebrafish. *Cell Rep.* **24**, 130–141 (2018).

35. Herbomel, P., Thisse, B. & Thisse, C. Ontogeny and behaviour of early macrophages in the zebrafish embryo. *Development* **126**, 3735–3745 (1999).

36. Herbomel, P., Thisse, B. & Thisse, C. Zebrafish Early Macrophages Colonize Cephalic Mesenchyme and Developing Brain, Retina, and Epidermis through a M-CSF Receptor-Dependent Invasive Process. *Dev. Biol.* **238**, 274–288 (2001).

37. Xu, J. *et al.* Temporal-Spatial Resolution Fate Mapping Reveals Distinct Origins for Embryonic and Adult Microglia in Zebrafish. *Dev. Cell* **34**, 632–641 (2015).

38. Peri, F. & Nüsslein-Volhard, C. Live Imaging of Neuronal Degradation by Microglia Reveals a Role for v0-ATPase a1 in Phagosomal Fusion In Vivo. *Cell* **133**, 916–927 (2008).

39. Bates, J. M. *et al.* Distinct signals from the microbiota promote different aspects of zebrafish gut differentiation. *Dev. Biol.* **297**, 374–386 (2006).

40. Parichy, D. M., Elizondo, M. R., Mills, M. G., Gordon, T. N. & Engeszer, R. E. Normal table of postembryonic zebrafish development: Staging by externally visible anatomy of the living fish. *Dev. Dyn.* **238**, 2975–3015 (2009).

41. Neuhauss, S. C. F. *et al.* Genetic Disorders of Vision Revealed by a Behavioral Screen of 400 Essential Loci in Zebrafish. *J. Neurosci.* **19**, 8603–8615 (1999).

42. Tabor, K. M. *et al.* Presynaptic Inhibition Selectively Gates Auditory Transmission to the Brainstem Startle Circuit. *Curr. Biol.* **28**, 2527-2535.e8 (2018).

43. Sholl, D. A. Dendritic organization in the neurons of the visual and motor cortices of the cat. *J. Anat.* **87**, 387–406 (1953).

44. Kunst, M. *et al.* A Cellular-Resolution Atlas of the Larval Zebrafish Brain. *Neuron* **103**, 21-38.e5 (2019).

45. Bates, A. S. *et al.* The natverse, a versatile toolbox for combining and analysing neuroanatomical data. *Elife* **9**, (2020).

46. Xu, J., Wang, T., Wu, Y., Jin, W. & Wen, Z. Microglia Colonization of Developing Zebrafish Midbrain Is Promoted by Apoptotic Neuron and Lysophosphatidylcholine. *Dev. Cell* **38**, 214–222 (2016).

47. Nimmerjahn, A. Resting Microglial Cells Are Highly Dynamic Surveillants of Brain Parenchyma in Vivo. *Science (80-.).* **308**, 1314–1318 (2005).

48. Paolicelli, R. C. *et al.* Synaptic pruning by microglia is necessary for normal brain development. *Science* **333**, 1456–1458 (2011).

49. Wake, H., Moorhouse, A. J., Jinno, S., Kohsaka, S. & Nabekura, J. Resting Microglia Directly Monitor the Functional State of Synapses In Vivo and Determine the Fate of Ischemic Terminals. *J. Neurosci.* **29**, 3974–3980 (2009).

50. Neufeld, K. M., Kang, N., Bienenstock, J. & Foster, J. A. Reduced anxiety-like behavior and central neurochemical change in germ-free mice. *Neurogastroenterol. Motil.* **23**, 255-e119 (2011).

51. Luczynski, P. *et al.* Microbiota regulates visceral pain in the mouse. *Elife* **6**, e25887 (2017).

52. Luczynski, P. *et al.* Adult microbiota-deficient mice have distinct dendritic morphological changes: differential effects in the amygdala and hippocampus. *Eur. J. Neurosci.* **44**, 2654–2666 (2016).

53. Clarke, G. *et al.* The microbiome-gut-brain axis during early life regulates the hippocampal serotonergic system in a sex-dependent manner. *Mol. Psychiatry* **18**, 666–673 (2013).

54. Guida, F. *et al.* Antibiotic-induced microbiota perturbation causes gut endocannabinoidome changes, hippocampal neuroglial reorganization and depression in mice. *Brain. Behav. Immun.* **67**, 230–245 (2018).

55. Sudo, N. *et al.* Postnatal microbial colonization programs the hypothalamic-pituitary-adrenal system for stress response in mice. *J. Physiol.* **558**, 263–275 (2004).

56. Sgritta, M. *et al.* Mechanisms Underlying Microbial-Mediated Changes in Social Behavior in Mouse Models of Autism Spectrum Disorder. *Neuron* **101**, 246-259.e6 (2019).

57. Varian, B. J. *et al.* Microbial lysate upregulates host oxytocin. *Brain. Behav. Immun.* **61**, 36–49 (2017).

58. Tabouy, L. *et al.* Dysbiosis of microbiome and probiotic treatment in a genetic model of autism spectrum disorders. *Brain. Behav. Immun.* **73**, 310–319 (2018).

59. Landin, J. *et al.* Oxytocin Receptors Regulate Social Preference in Zebrafish. *Sci. Rep.* **10**, 5435 (2020).

60. Gunaydin, L. A. & Deisseroth, K. Dopaminergic dynamics contributing to social behavior. *Cold Spring Harb. Symp. Quant. Biol.* **79**, 221–227 (2014).

61. Geng, Y. & Peterson, R. T. The zebrafish subcortical social brain as a model for studying social behavior disorders. *DMM Disease Models and Mechanisms* vol. 12 (2019).

62. Teles, M. C., Dahlbom, S. J., Winberg, S. & Oliveira, R. F. Social modulation of brain monoamine levels in zebrafish. *Behav. Brain Res.* **253**, 17–24 (2013).

63. Du, Y. *et al.* Spatial and temporal distribution of dopaminergic neurons during development in zebrafish. *Front. Neuroanat.* **10**, 1–7 (2016).

64. Erny, D. *et al.* Host microbiota constantly control maturation and function of microglia in the CNS. *Nat. Neurosci.* **18**, 965–977 (2015).

65. Wu, S. *et al.* Il34-Csf1r Pathway Regulates the Migration and Colonization of Microglial Precursors. *Dev. Cell* **46**, 552-563.e4 (2018).

66. Westerfield, M. The Zebrafish Book. A Guide for the Laboratory Use of Zebrafish (Danio rerio), 5th Edition. *Univ. Oregon Press. Eugene* (2007).

67. Melancon, E. *et al.* Best practices for germ-free derivation and gnotobiotic zebrafish husbandry. in *The Zebrafish - Disease Models and Chemical Screens* vol. 138 61–100 (Elsevier, 2017).

68. Larsch, J. & Baier, H. Biological Motion as an Innate Perceptual Mechanism Driving Social Affiliation. *Curr. Biol.* **28**, 3523-3532.e4 (2018).

69. Susaki, E. A. *et al.* Advanced CUBIC protocols for whole-brain and whole-body clearing and imaging. *Nat. Protoc.* **10**, 1709–1727 (2015).

70. Schindelin, J. *et al.* Fiji: an open-source platform for biological-image analysis. **9**, 676–682 (2012).